



Deposited via The University of Leeds.

White Rose Research Online URL for this paper:

<https://eprints.whiterose.ac.uk/id/eprint/173301/>

Version: Accepted Version

Article:

Greer, AJ, Taylor, SFR, Daly, H et al. (2021) Combined Experimental and Theoretical Study of the Competitive Absorption of CO₂ and NO₂ by a Superbase Ionic Liquid. ACS Sustainable Chemistry and Engineering, 9 (22). pp. 7578-7586. ISSN: 2168-0485

<https://doi.org/10.1021/acssuschemeng.1c01451>

Reuse

Items deposited in White Rose Research Online are protected by copyright, with all rights reserved unless indicated otherwise. They may be downloaded and/or printed for private study, or other acts as permitted by national copyright laws. The publisher or other rights holders may allow further reproduction and re-use of the full text version. This is indicated by the licence information on the White Rose Research Online record for the item.

Takedown

If you consider content in White Rose Research Online to be in breach of UK law, please notify us by emailing eprints@whiterose.ac.uk including the URL of the record and the reason for the withdrawal request.

Combined Experimental and Theoretical Study of the Competitive Absorption of CO₂ and NO₂ by a Superbase Ionic Liquid

Adam J. Greer^{†,‡,}, S. F. Rebecca Taylor[‡], Helen Daly[‡], Matthew G. Quesne^{#,‡}, Nora H. de
Leeuw^{#,‡}, C. Richard A. Catlow^{#,‡}, Johan Jacquemin^{§,v,*}, Christopher Hardacre^{‡,*}*

[†] School of Chemistry and Chemical Engineering, Queen's University Belfast, David Keir
Building, Stranmillis Road, Belfast, BT9 5AG, Northern Ireland

[‡] Department of Chemical Engineering and Analytical Science, The University of
Manchester, The Mill, Sackville Street, Manchester, M13 9PL, United Kingdom

[#] School of Chemistry, Cardiff University, Main Building, Park Place, Cardiff, CF10 3AT,
United Kingdom

[‡] UK Catalysis Hub, Research Complex at Harwell, STFC Rutherford Appleton Laboratory,
Didcot, Oxfordshire, OX11 0FA, United Kingdom

[‡] School of Chemistry, University of Leeds, Leeds, LS2 9JT, United Kingdom

[§] Université de Tours, Laboratoire PCM2E, Parc de Grandmont, 37200, Tours, France

^v Materials Science and Nano-Engineering, Mohammed VI Polytechnic University, Lot 660-
Hay Moulay Rachid, Ben Guerir 43150, Morocco

AUTHOR INFORMATION

Co-Corresponding Authors:

* Christopher Hardacre, Tel: +44 (0) 161 306 2672, E-mail: c.hardacre@manchester.ac.uk

* Johan Jacquemin, Tel: +33 (0) 2 47 36 73 29, Fax: +33 (0) 2 47 36 70 73, E-mail: jj@univ-tours.fr

* Adam Greer, Tel: +44 (0) 161 306 2227, E-mail: adam.greer@manchester.ac.uk

Abstract

A superbase ionic liquid (IL), trihexyltetradecylphosphonium benzimidazolide ([P₆₆₆₁₄][Benzim]), is investigated for the capture of CO₂ in the presence of NO₂ impurities. The effect of the waste gas stream contaminant on the ability of the IL to absorb simultaneously CO₂ is demonstrated using novel measurement techniques, including a mass spectrometry breakthrough method and *in-situ* infrared spectroscopy. The findings show that the presence of an industrially relevant concentration of NO₂ in a combined feed with CO₂ has the effect of reducing the capacity of the IL to absorb CO₂ efficiently by ~60% after 10 absorption-desorption cycles. This finding is supported by physical property analysis (viscosity, ¹H and ¹³C NMR, XPS), and spectroscopic infrared characterization, in addition to density functional theory (DFT) calculations, to determine the structure of the IL-NO₂ complex. The results are presented in comparison with another flue gas component, NO, demonstrating that the absorption of NO₂ is more favorable, thereby hindering the ability of the IL to absorb CO₂. Significantly, this work aids understanding of the effects that individual components of flue gas have on CO₂ capture sorbents, through studying a contaminant that has received limited interest previously.

Keywords: Ionic liquids; CO₂ capture; NO₂; flue gas; competitive absorption; infrared; DFT

Introduction

Post-combustion CO₂ capture is an important requirement of many industrial processes. The high-temperature combustion of fossil fuels produces large quantities of CO₂ (10-15 vol.%), as well as other impurities, such as SO₂ (0.05-0.2 vol.%) and NO_x (0.15-0.25 vol.%) which consists predominantly of NO and NO₂. [1–3] The reported values are before any desulfurization or denitrification technologies. In particular, NO_x is known to have significant impact on health and the environment, causing the formation of atmospheric ozone and acid rain. [4] It is therefore vital that NO_x emissions are regulated (40 µg·m⁻³ a year), leading to the fitting of NO_x scrubbers to power stations, comprising oxidizing and reducing agents responsible for the conversion of NO_x to N₂. [5] Aqueous alkanolamines have been employed as CO₂ capture sorbents, but the presence of NO_x was found to result in the irreversible formation of carcinogenic nitrosamines and a decrease in CO₂ capture efficiency. [6–8] Ionic liquids (ILs) have also been widely investigated for the capture of CO₂ as a non-volatile alternative to toxic alkanolamines. However, to date, the effect of NO₂ on the ability of an IL to capture CO₂ in a combined feed has not been investigated.

The interest in ILs stems from the ability to alter their physiochemical properties, such as their thermal stability or CO₂ absorption capacity, through changing the combination of cation and anion, allowing the tuning of their properties for specific applications. [9,10] For example, the amount of CO₂ absorbed by a particular IL has been shown to have a strong dependence on the anion, with conventional anions only physically absorbing small quantities of CO₂, [11,12] compared with task-specific ILs that incorporate amine functionality and chemically absorb up to 1 nCO₂:nIL. [13,14] Superbase ILs (SBILs) containing an aprotic heterocyclic anion (AHA) were developed to minimize the increase in viscosity observed in amine-functionalized ILs, and they can reversibly capture a greater than equimolar amount of CO₂. [15–18] Extensive studies into the absorption of other acidic gases such as SO₂ and NO

by SBILs have found that irreversible absorption was observed in many cases, often on multiple active sites within the IL, affecting the recyclability of the system.[19–25]

The effect of impurities on the CO₂ uptake of the SBIL trihexyltetradecylphosphonium benzimidazolide, [P₆₆₆₁₄][Benzim], has previously been investigated in combined feeds. SO₂ was shown to deactivate the IL through binding to the absorption site available to CO₂, while the presence of NO exhibited little effect on the IL's capacity for the uptake of CO₂. [26,27] For NO, the co-binding of CO₂ and NO as carbamate and NONO-ate species, respectively, was observed at different N-sites of the benzimidazolide anion. However, competition for the same binding site was reported between CO₂ and SO₂ which markedly influenced the absorption capacity and recyclability of the IL. The differing effects of SO₂ and NO on the absorption of CO₂ by [P₆₆₆₁₄][Benzim] highlight the need to assess the components of flue gas impurities, both individually and in combination with CO₂.

The capture of NO₂ by ILs has been the focus of only a few studies, where it was found that an increased uptake is observed for NO₂ compared to NO. [28–30] To date, NO₂ has not been studied in a combined feed with CO₂, so its direct influence on the ability of a sorbent to capture CO₂ is unknown. The competitive absorption of CO₂ with industrially relevant concentrations of H₂O, SO₂ or NO, independently, has been investigated previously in [P₆₆₆₁₄][Benzim], and this IL was therefore selected for the current study to gain a comprehensive insight into more complex, multi-component feeds. [18,26,27] The use of a recently developed analytical method utilizing mass spectrometry, [26] allows the study of this superbase IL under realistic, dry, flue gas conditions with a feed containing 14% CO₂ and 0.2% NO₂. Further molecular level information was provided by Density Functional Theory (DFT) calculations and spectroscopic data (NMR, IR and XPS).

Experimental

Materials

Trihexyltetradecylphosphonium chloride ([P₆₆₆₁₄]Cl, 97.7 wt.%, CAS: 258864-54-9) was procured from IoLiTec, and benzimidazole (98 wt.%, CAS: 51-17-2) was purchased from Sigma–Aldrich. [P₆₆₆₁₄][Benzim] was prepared using a two-step synthesis method reported previously.[18] The halide content was determined to be <5 ppm using a silver nitrate test.[31] Water content was measured to be <0.1 wt.% using a Metrohm 787 KF Titrino Karl Fischer machine. The structure and purity of the IL, after synthesis and post-absorption, was analyzed using ¹H-NMR and ¹³C-NMR with a Bruker Avance II 400 MHz Ultra shield Plus, and carried out as neat ILs in the presence of a glass capillary insert containing deuterated solvent (DMSO-d₆, purchased from Cambridge Isotope Laboratories Inc., CAS: 2206-27-1). Gases were obtained from BOC; argon (99.998%, CAS: 7440-37-1); carbon dioxide (99.99%, CAS: 124-38-9); nitrogen dioxide (1% in argon, CAS: 10102-44-0).

Methods

The gas absorption measurement techniques used in this work were reported in detail previously, and the same protocol was followed in this work.[26,27] To briefly summarize this; the uptake of a single component gas feed (1% NO₂ in argon) by [P₆₆₆₁₄][Benzim] was studied gravimetrically at 22 ± 0.5 °C. A mass spectrometer based method was utilized to study the gas phase concentrations at the outlet after the IL was exposed to a mixed gas feed of 14% CO₂ + 0.2% NO₂ in Ar. A series of cycles were performed consisting of a 2 h absorption period at 22 °C, followed by a 2 h desorption period under Ar at 90 °C for 2 h.

Analysis

The viscosity of the IL samples was measured before and after NO₂ absorption using a TA Instruments AR2000. Elemental analysis was carried out using a Thermo Scientific Flash 2000 elemental analyzer. X-ray Photoelectron Spectroscopy (XPS) was performed with a Kratos AXIS Ultra DLD apparatus, with monochromated Al K α radiation X-ray source, charge neutralizer and hemispherical electron energy analyzer. During data acquisition, the chamber pressure was kept below 10⁻⁹ mbar. The spectra were analyzed using CasaXPS and corrected for charging using the C 1s feature at 284.8 eV.

Attenuated Total Reflectance-Infrared (ATR-IR) spectra were recorded in a modified *in-situ* cell with a ZnSe crystal and a PIKE ATRMax II accessory housed in a Bruker Tensor II infrared spectrometer. A thin film of [P₆₆₆₁₄][Benzim] (~250 mg) coated the ZnSe crystal in the cell before introduction of the gas feed (14% CO₂ in Ar, 0.2% NO₂ in Ar, or a mixed gas feed of 14% CO₂ with 0.2% NO₂ in Ar) with a flow rate of 15 cm³·min⁻¹ at 22 °C. Desorption was performed at 90 °C under Ar. The background for all spectra was the ZnSe crystal in the cell and spectra were recorded with 8 scans at 4 cm⁻¹ resolution. The spectrum of the IL before introduction of the gas feed has been subtracted from all the spectra of the IL under gas absorption.

DFT Calculations

DFT calculations followed a similar protocol to previous work on this system and whilst a brief overview will be included here, a more detailed description can be found in the literature.[27] Calculations were performed with the Gaussian09 software package,[32] using a combination of the hybrid functional UB3LYP and the triplet- ζ basis set 6-311+G*, as reported in previous work.[33–35] Starting geometries for [P₃₃₃₃][Benzim] models were also informed by previous molecular dynamical studies,[36] with absorbates manually added using the ChemCraft software package.[37] Minima structures for all possible reaction mechanisms

were fully optimized without constraints with transition states located by initially running geometry scans, where only the degree of freedom connecting two minima was fixed. Full transition state optimizations were subsequently performed on the highest energy structures obtained along each reaction coordinate. Verification of both minima and transition states were carried out with the aid of analytical frequencies at 1 atm and 298.15 K, whereby, only positive frequencies were observed for each minima, with each transition state possessing a single imaginary frequency for the mode associated with the reaction coordinate. Corrections for long range interactions were included with the aid of the Grimme D3 dispersion model,[38] whilst solvent effects were simulated with an implicit model of acetonitrile ($\epsilon = 35.688$), using a Polarizable Continuum Model (PCM).

Results and Discussion

The absorption of 1% NO₂ in Ar by [P₆₆₆₁₄][Benzim] was initially examined using a gravimetric technique to allow direct comparison with the literature on the uptake of individual gases. It was found that an average of 4.60 nNO₂:nIL was absorbed at saturation (Figure S1), with the higher than equimolar capacity indicating a multi-site absorption effect for NO₂, as was found for NO.[27] The amount of NO₂ absorbed far exceeds that found for 1% NO by the same IL (1.73 nNO:nIL), indicating a different mechanism of absorption for NO₂. [27] The regeneration of the IL at 90 °C (well below the IL's decomposition temperature of 289 °C)[18] under argon was studied, with 3.64 nNO₂:nIL remaining after 2 hours. NO₂ absorption is evidently not a reversible process, with the absorbed species strongly bound to the IL, which has also been observed for caprolactam-based ILs.[28]

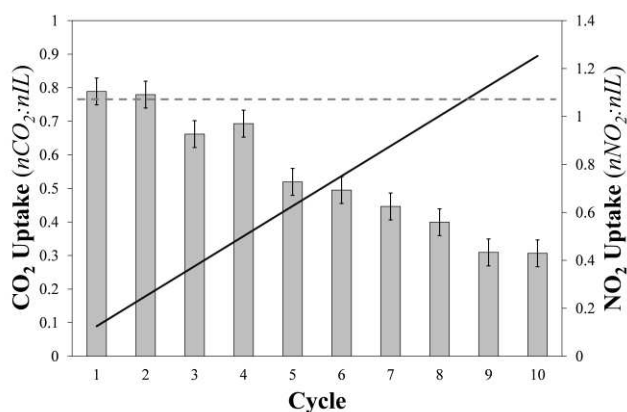


Figure 1. CO₂ capacity (bars) of [P₆₆₆₁₄][Benzim], calculated from the MS (± 0.04 nCO₂:nIL), and calculated exposure to NO₂ (solid line), after multiple cycles of a 2 h absorption under a feed 14% CO₂ and 0.2% NO₂ in argon, and a 2 h desorption at 90 °C. Dashed line depicts the 14% CO₂ only value (0.78 nCO₂:nIL).

The ability of NO₂ to compete with CO₂ for absorption by [P₆₆₆₁₄][Benzim] was investigated using a combined feed through a series of absorption and desorption cycles, employing a mass spectrometry-based gas absorption rig.[26] Realistic flue gas concentrations of 14% CO₂ and 0.2% NO₂ were selected, with the results shown in Figure 1 (and Table S1). It demonstrates that after two cycles in the gas absorption rig, the CO₂ capacity of the IL was unaffected by the presence of NO₂, with 0.78 nCO₂:nIL still absorbed. After the third cycle, a clear decrease in CO₂ capacity was observed, with 0.66 nCO₂:nIL absorbed after exposure to a calculated 0.38 nNO₂:nIL. The ability of [P₆₆₆₁₄][Benzim] to capture CO₂ in the presence of NO₂ continued to decrease, reaching 0.31 nCO₂:nIL after 10 absorption/desorption cycles, a ~60% reduction in capacity. It was evident that the desorption conditions (2 h under Ar at 90 °C) were unable to regenerate the original CO₂ capacity. This strong irreversible absorption of NO₂ is in contrast to the behavior observed with the NO co-feed, where 0.72 nCO₂:nIL was still absorbed after 10 cycles.[27]

Following the 10 competitive absorption/desorption cycles with CO₂ and NO₂, the treated IL was characterized using a number of techniques. Elemental analysis showed an increase in the nitrogen content of [P₆₆₆₁₄][Benzim], from 6.10 to 7.67 wt.%, and an increase in the viscosity from 1087 to 1516 mPa·s (at 25 °C). These changes were assigned to the irreversible incorporation of nitrogen into the IL through the absorption of NO₂. Changes in the physical properties of the IL after exposure to NO₂ were more significant than those observed after exposure to NO (nitrogen content increased from 6.10 to 6.48%, and viscosity from 1087 to 1235 mPa·s), correlating with the reduced effect of the NO impurity (0.72 nCO₂:nIL was still absorbed after 10 cycles under NO and CO₂).^[27] As the irreversible absorption of NO₂ causes changes in the physical properties of the IL, NMR and XPS of the IL after exposure were performed to characterize the nature of the strongly bound NO₂ species.

The structure was initially probed using ¹H NMR (Figure S2), where it was expected that changes in the spectra upon the absorption of NO₂ would be caused by a change in the environment of the protons in the heterocyclic anion, which was demonstrated by a downfield shift in the peaks at 6.34/6.91/7.36 ppm (a) to 6.57/7.10/7.65 ppm (b) after the IL was treated with 1% NO₂ for 24 h, similar to shifts observed with SO₂ and NO.^[26,27] The IL from the absorption rig after the final cycle (c) displayed a similar shift, showing that the same absorbed species was formed under the different conditions. In both spectra after NO₂ exposure, new peaks were observed above 13 ppm, suggesting the formation of HNO₃ from the reaction of NO₂ with residual water in the IL. The formation of HNO₃ was further confirmed by IR spectroscopy of [P₆₆₆₁₄][Benzim] after 24 h exposure to 1% NO₂ (Figure S4). The ¹³C NMR spectra (Figure S3) showed analogous changes, where small shifts were noted for the peaks attributed to the benzimidazolide anion (114-148 ppm), due to changes in aromaticity caused by NO₂ absorption.

Ex-situ XPS was further used to characterize the IL post-exposure in the absorption rig. A comparison of the N 1s region showed the presence of two new N 1s photoelectron peaks at 402.0 and 406.1 eV assigned to N-O species (Figure S5). The broad peak at 402.0 eV is assigned to absorbed NO₂, with the peak at a higher binding energy of 406.1 eV indicating a more oxidized N species, which can be attributed to N₂O₄ absorption.[39,40] Absorption of NO in the same IL resulted in a single photoelectron peak observed at 402.4 eV which was attributed to N₂O₂ formation.[27,41] These species are expected to be strongly absorbed to the IL, as the high vacuum in the XPS analyzing chamber would negate the detection of any weakly absorbed gases.

ATR-IR spectra of [P₆₆₆₁₄][Benzim] under separate CO₂ or NO feeds have been reported previously, showing characteristic bands for the absorbed species, with additional changes in the spectra observed due to changes in the aromaticity of the [Benzim]⁻ anion.[27] For CO₂, reversible absorption and an equimolar capacity for absorption presented a simpler system than that for multi-site absorption, which has been reported here for NO₂, and NO.[27] With the higher absorption capacity of [P₆₆₆₁₄][Benzim] for NO₂ and the formation of a strongly bound species, a combined approach using theoretical DFT calculations and FTIR was utilized to investigate the nature of the absorbed species in [P₆₆₆₁₄][Benzim].

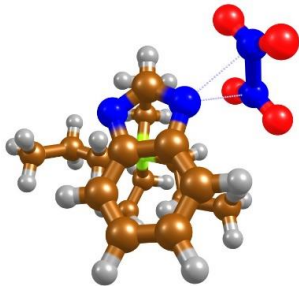
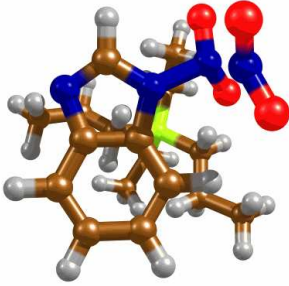
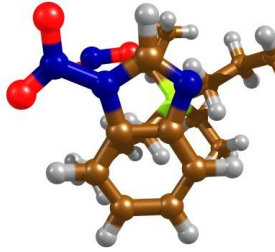
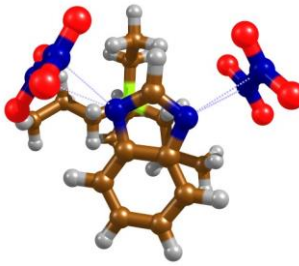
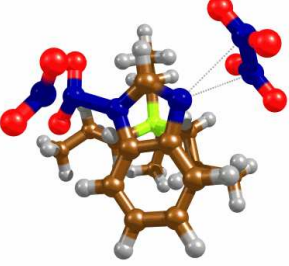
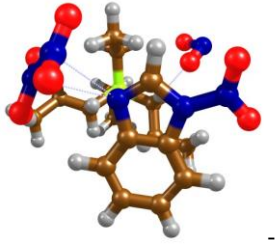
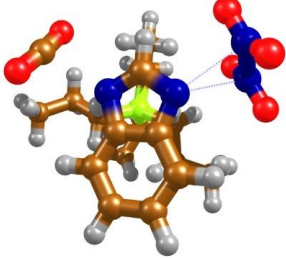
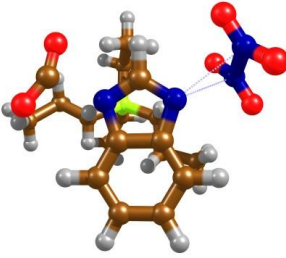
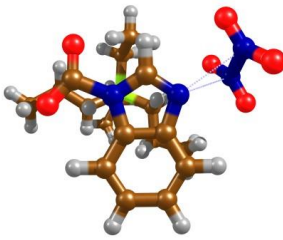
DFT calculations revealed that the formation of an N₂O₄ dimer, physically absorbed to the [Benzim]⁻ anion, was the most thermodynamically favored absorption mode (Table 1 (a)). The charge perturbation from the [Benzim]⁻ anion strongly enhanced the rate of dimerization of NO₂, pushing the equilibrium towards N₂O₄ formation by strongly absorbing the dimer and thus removing it from the gas phase. The N₂O₄ dimer was found to physically absorb strongly to the [Benzim]⁻ anion, with a zero-point corrected absorption enthalpy (E_{ZPE}) of -107.8 kJ·mol⁻¹ (Table S2-S3). Although the absorption of N₂O₄ is energetically very favorable, the absorbed geometry together with a detailed comparison of grouped Mulliken charges (Table S4-S5)

indicates that it is a purely physical process without charge transfer from the anion, in comparison to that of chemically absorbed CO₂. Instead, there are extremely strong dipole interactions between the two δ⁺ nitrogen centers of the absorbate, and the formal negative charge on the anion.

Furthermore, the physical absorption of two N₂O₄ dimers at both N-sites of the [Benzim]⁻ anion was energetically favorable, with an absorption enthalpy of -210.5 kJ·mol⁻¹ (Table 1 (c)). The multi-site absorption and greater than equimolar absorption of NO₂ to the IL correlates with the large gravimetric uptake capacity (4.60 nNO₂:nIL), and the high absorption enthalpies relate to the drop in CO₂ capacity observed. These findings are also consistent with the experimentally observed results, where only a small decrease in absorbed NO₂ was observed after desorption, probably due to the loss of weaker, physically bound, NO₂.

ATR-IR spectra recorded during the absorption of 0.2% NO₂ in Ar by [P₆₆₆₁₄][Benzim] are shown in Figure 2. It is evident that upon the introduction of NO₂, a series of overlapping bands in the 1300-1400 cm⁻¹ region increased in intensity. Interestingly, upon initial exposure to the feed, a band at 1335 cm⁻¹ was the most intense in this region, but with increasing exposure time, a band at 1315 cm⁻¹ dominated the spectra. In addition, bands at 1620, 1233 and 1036 cm⁻¹ increased in intensity with exposure to the NO₂ feed. These changing bands could indicate a change in the nature of the absorbed species, or absorption of a NO₂ species at another N-site on the [Benzim]⁻ anion, as was observed with NO.[27]

Table 1. Reaction landscapes showing intermediates (I) and transition states (TS) for N₂O₄ and N₂O₄/CO₂ absorption by [P₃₃₃₃][Benzim], depicting potential energy surfaces for (a) absorption of N₂O₄, and subsequent heterolytic cleavage of the N-N bond, (b) absorption of two moles of N₂O₄, and the barrier to cleavage of the N-N bond, and (c) the absorption of CO₂ by [Benzim-N₂O₄]. Values are given in kJ·mol⁻¹ with zero-point corrected gas phase and {solvent} corrected energies calculated at B3LYP/6-311+G* level of theory (*pseudo bonds* = *physisorption*, *solid bonds* = *chemisorption*).

Absorbate	Intermediate/ I ₁ (kJ·mol ⁻¹)	Transition State/ TS (kJ·mol ⁻¹)	Intermediate/ I ₂ (kJ·mol ⁻¹)
N ₂ O ₄	(a) [Benzim] ⁻ ...N ₂ O ₄  -107.82 {-85.69}	 -66.23 {-65.78}	(b) [Benzim-NO ₂] ⁻ + [NO ₂] ⁻  162.29 {-137.54}
	(c) [Benzim] ⁻ ...(N ₂ O ₄) ₂  -210.53 {-174.52}	 -158.64 {-154.11}	(d) [Benzim] ⁻ ...(N ₂ O ₄) ₂  231.11 {-215.89}
	(e) [Benzim] ⁻ ...N ₂ O ₄ ...CO ₂  -137.39 {-102.60}	 -131.28 {-99.13}	(f) [Benzim-CO ₂] ⁻ ...N ₂ O ₄  -147.32 {-131.15}

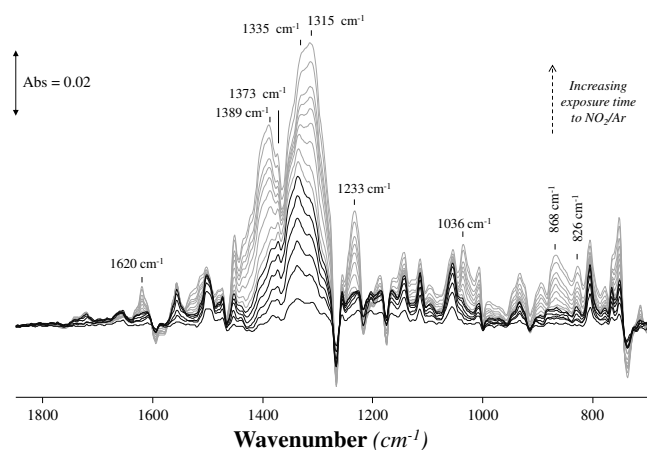


Figure 2. ATR-IR spectra of [P₆₆₆₁₄][Benzim] exposed to a feed of 0.2% NO₂ in Ar from 0 to 2 mins. The spectrum of the IL before introduction of NO₂ has been subtracted from all spectra recorded under the NO₂ feed. Studied at 22 °C with a flow rate of 15 cm³·min⁻¹.

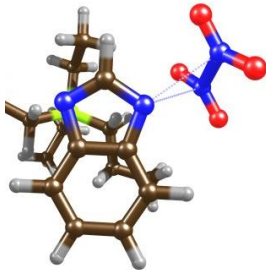
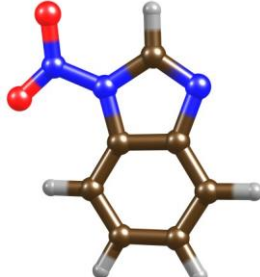
Calculated vibrational spectra for one or two moles of physisorbed N₂O₄ to N-sites on the [Benzim]⁻ anion showed indistinguishable spectral profiles, with theoretically derived bands at 1426, 1308 and 847 cm⁻¹ for one mole of physically absorbed N₂O₄ (Table 2), and 1433-1427, 1313-1305 and 847 cm⁻¹ for two moles of N₂O₄. The bands which formed upon introduction of NO₂ at 868, 1335 and 1373 cm⁻¹ correspond with the calculated bands for physisorbed N₂O₄ (Table 2). Bands at 1764/68 and 1825/24 cm⁻¹ were predicted for the $\nu_{\text{asym}}(\text{O-N-O})$ vibration when one/two moles of N₂O₄ were physically absorbed, but these bands were not observed experimentally, as described by other authors.[42–44]

While physisorbed N₂O₄ was observed initially, the spectra showed changes with time on stream which were not simply an increase in intensity of the bands assigned to N₂O₄, thus suggesting evolution of the absorbed species with increasing NO₂ concentration. The N-N bond of absorbed N₂O₄ has been reported to undergo heterolytic cleavage, forming [NO₃]⁻ and [NO]⁺ ionic species, due to perturbation by an external charged species (Equation 1).[45,46] The energy diagrams in Table 1 show the most favored reaction pathway following the physisorption of one and two moles of N₂O₄, respectively. In these reaction schemes,

heterolytic cleavage of the N-N bond of absorbed N_2O_4 is favorable (b), but the activation barrier for the disproportionation reaction to $\text{NO}^+/\text{NO}_3^-$ was above 100 kJ mol^{-1} and was considered too high (Figure S6). Cleavage of the N-N bond to form $[\text{NO}_2]^+$ and $[\text{NO}_2]^-$, however, can occur owing to the lower barrier ($41.6 \text{ kJ}\cdot\text{mol}^{-1}$), forming a thermodynamically stable complex, which is the favored theoretical pathway following the initial physisorption of N_2O_4 on $[\text{P}_{66614}][\text{Benzim}]$.



Table 2. Depicts the experimental and [theoretical] IR vibrations measured when $[\text{P}_{66614}][\text{Benzim}]$ is exposed to NO_2 .

Species	Vibration	IR vibration (cm^{-1})
(a) $[[\text{Benzim}] \dots [\text{N}_2\text{O}_4]]$		
	$\nu(\text{N-N})$	868 [847]
	$\nu_s(\text{O-N-O})$	1335 [1308]
	$\nu(\text{N}_2\text{O}_4)$	1373 [1426]
	$\nu_{\text{as}}(\text{O-N-O})$	1772/1825
		[1764/1825]
(b) $[\text{Benzim-NO}_2]$		
	$\nu(\text{O-N-O})$	868 [843]
	$\nu(\text{N-N})$	1036 [1071]
	$\nu_s(\text{O-N-O})$	1308 [1312-47]
	$\nu_{\text{as}}(\text{O-N-O})$	1620 [1630-76]

(c) [P_{RRRR}][NO₂]

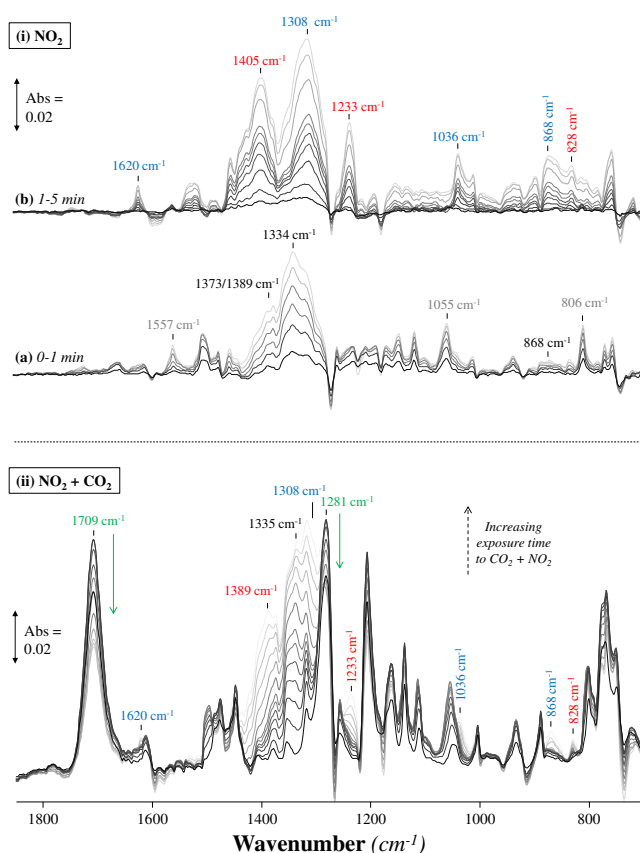


$\nu(\text{O-N-O})$	828 [816]
$\nu_s(\text{O-N-O})$	1233 [1236]
$\nu_{as}(\text{O-N-O})$	1405 [1383]

The theoretical pathway involving [NO₂]⁺ and [NO₂]⁻ species has significant implications for the absorption capacity of the IL. The [NO₂]⁺ ion is proposed to absorb chemically to the [Benzim]⁻ anion, leading to a neutral [Benzim-NO₂] complex (Table 2 (b)). The neutralization of the [Benzim]⁻ anion removes the active site for absorption, causing deactivation of the anion/IL and providing evidence for the decreased CO₂ capacity. The [NO₂]⁻ ion stabilizes the positively charged [P₃₃₃₃]⁺ cation by orienting the negatively charged oxygen atoms into a position to counter the positively charged phosphorus (Table 2 (c)). It could be proposed that the [NO₂]⁻ ion reacts with, or deprotonates, the acidic α -protons close to the phosphonium cation center (P-CH₂-), but this pathway was not observed (see Table 2 (c) which shows the lowest energy structure).[47] Additionally, Table 1 (c-d) shows that when two moles of N₂O₄ are physically bound, which is more likely at increased exposure times, the heterolytic cleavage of the N-N bonds has little driving force due to similar initial and final state energies, as well as a higher barrier (51.9 kJ·mol⁻¹). Thus, the formation of the neutral [Benzim-NO₂] complex (d) is expected to be equilibrium-limited, leading to the gradual decrease in the CO₂ capacity of the IL.

To probe the evolution of the bands in Figure 2, the spectrum after 1 minute under the NO₂ feed was subtracted from all subsequent spectra (Figure 3) to allow comparison with the theoretically determined band positions of the [Benzim-NO₂]/[P_{RRRR}][NO₂] complexes (Table 2). A new band was observed at 1233 cm⁻¹, attributed to the formation of a [NO₂]⁻ anion, and related to vibrations at 1405 and 828 cm⁻¹. Evidence of a new N-N bond was observed at 1036

cm^{-1} , from the formation of the neutral $[\text{Benzim-NO}_2]$ complex, associated with bands at 1620, 1308 and 868 cm^{-1} . [48–50] The DFT calculated species correlated well with the observed ATR



spectra, and additional features were due to changes in the aromaticity of the $[\text{Benzim}]^-$ anion, as observed with $\text{CO}_2/\text{SO}_2/\text{NO}$. [26,27] Interestingly, the changes in the anion aromaticity are observed during the physical absorption of N_2O_4 , showing that the strong initial interaction distorts the charge density of the anion.

Figure 3. ATR-IR spectra of $[\text{P}_{66614}][\text{Benzim}]$ exposed to a feed of (i) 0.2% NO_2 in Ar after (a) 1 minute, and (b) between 1 and 5 minutes with subtraction of the spectrum recorded at 1 minute; and (ii) 14% $\text{CO}_2 + 0.2\%$ NO_2 in Ar, for 0-2 mins. Studied at $22 \text{ }^\circ\text{C}$ with a flow rate of $15 \text{ cm}^3 \cdot \text{min}^{-1}$. The color of the labelled bands indicates physisorbed N_2O_4 (**black**), changes in the aromaticity of the IL (**grey**), chemical absorption of CO_2 (**green**), $[\text{Benzim-NO}_2]$ (**blue**), and $[\text{P}_{66614}][\text{NO}_2]$ (**red**).

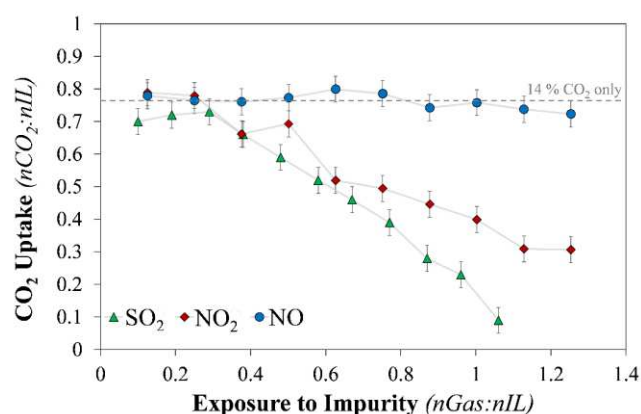
Combining both the DFT calculations and the FTIR spectroscopic study allowed the determination of the absorbed species, and how the speciation changes with time. The DFT results indicate the thermodynamically stable intermediates, while FTIR provides evidence for the proposed intermediates and the kinetics of absorption. Together, the results indicate the strong physical absorption of N_2O_4 , followed by the deactivation of the IL through the formation of $[Benzim-NO_2]/[P_{RRRR}][NO_2]$ complexes at increased exposure times, which would be expected to result in a loss of absorption sites for CO_2 and the co-absorption of CO_2 was therefore studied as well.

A co-feed of 14% CO_2 and 0.2% NO_2 in Ar was investigated, simulating conditions in the gas absorption rig (Figure 3 (ii)), to study whether bands assigned to the neutral complex would form and influence the CO_2 absorption capacity of the IL (as observed in the absorption rig results). The chemical absorption of CO_2 results in the formation of a carbamate species, with bands at 1709 (C=O) and 1281 cm^{-1} (N-COO⁻) quickly increasing during the first minute of exposure to the feed, which is caused by the greater concentration of CO_2 in the feed.[26] Simultaneously, bands associated with the physical absorption of N_2O_4 grow (1373 and 1334 cm^{-1}), due to the strong absorption enthalpy of the species (-107.8 $kJ\cdot mol^{-1}$). As the exposure time increases, the band at 1709 cm^{-1} (C=O) is noted to decrease, while weak bands at 1233, 1036, 868 and 828 cm^{-1} appear, indicating the chemical absorption of NO_2^+ to the [Benzim]⁻ anion and the formation of $[P_{66614}][NO_2]$. This correlates with the stepped reduction in CO_2 capacity observed in the gas absorption rig. Subtracted data in Figure S7 show that bands due to the heterolytic cleavage of physisorbed N_2O_4 are observed to form with and without the presence of CO_2 . The absorption of CO_2 does not hinder the absorption and subsequent heterolytic cleavage of N_2O_4 , which, however, deactivates the IL to further absorption of CO_2 .

The physical absorption of N_2O_4 at one site drastically changes the kinetics and thermodynamics of absorption at the remaining site, where the barrier for CO_2 activation is low

(6.1 kJ·mol⁻¹) (Table 1 (e-f)). Calculations show that the co-absorption of N₂O₄ and CO₂ to separate N-sites is thermodynamically stable (-147 kJ·mol⁻¹), aided by the low concentration of NO₂. After an extended period, both the deactivation of the [Benzim]⁻ anion, and the larger absorption enthalpy of the binding of two moles of N₂O₄ (-211 kJ·mol⁻¹), suggests that decreases in CO₂ capacity are observed due to the loss of absorption sites. The reaction mechanism between the IL and CO₂/NO₂ is depicted in Figure S9, showing how the binding of a second N₂O₄ dimer further deactivates [P₆₆₆₁₄][Benzim] for CO₂ capture, before formation of the [Benzim-NO₂]/[P_{RRRR}][NO₂] complexes occurs at increased exposure times. The irreversible nature of the bound species is further demonstrated through studying the regeneration of the IL at 90 °C (Figure S8), where it was clear that the NO_x species could not be fully desorbed from [P₆₆₆₁₄][Benzim].

These results differ from those when NO is in the co-feed, where co-absorption of both CO₂ and NO was observed.[27] The results obtained previously with NO were rationalized by the reaction landscape depicted in Figure S10, where the reduction of CO₂ is a barrierless process, and the activation barrier to form the NONO-ate complex is relatively high, showing a preference for the absorption of CO₂. After formation of the carbamate, slow deactivation of the IL is observed in the presence of NO *via* a CO₂ bond intermediate (which enables NO to co-bind). Using *in silico* techniques, this observation was explained by the relatively high kinetic barriers for the formation of the NO_x species bound to the IL from NO, as opposed to



NO₂. Therefore, it is evident that an alternative absorption mechanism occurs, accelerating the effect that NO₂ has on the uptake of CO₂.

Figure 4. CO₂ uptake of [P₆₆₆₁₄][Benzim] after exposure to an increasing amount of flue gas impurity ▲ SO₂; ◆ NO₂; ● NO; after multiple absorption/desorption cycles of a feed containing 14% CO₂ and 0.2% impurity; ---- 14% CO₂ only value. ▲ SO₂; Adapted with permission from Taylor, S. F. R., McClung, M., McReynolds, C., Daly, H., Greer, A. J., Jacquemin, J. & Hardacre, C. Understanding the Competitive Gas Absorption of CO₂ and SO₂ in Superbase Ionic Liquids. *Ind. Eng. Chem. Res.* **2018**, *57*, 17033–17042. Copyright 2018 American Chemical Society. ● NO; Adapted with permission from Greer, A. J., Taylor, S. F. R., Daly, H., Quesne, M., Catlow, C. R. A., Jacquemin, J. & Hardacre, C. Investigating the Effect of NO on the Capture of CO₂ Using Superbase Ionic Liquids for Flue Gas Applications. *ACS Sustain. Chem. Eng.* **2019**, *7*, 3567–3574. Copyright 2019 American Chemical Society.

A summary of the effect of the different waste gas stream impurities on [P₆₆₆₁₄][Benzim] studied here, is shown in Figure 4. It is clear that SO₂ has the greatest effect on reducing the CO₂ uptake in ILs, followed by NO₂ and finally NO, in clear accord with the calculated absorption energies of -124, -108, and -91 kJ·mol⁻¹, respectively (CO₂ = -52 kJ·mol⁻¹).[27] It should be noted, that whereas the formation of the NONO-ate is thermodynamically stable (from the absorption of NO), this process is kinetically slow, hindered by the high concentration of CO₂ in the gas feed.

Summary and Conclusions

The accelerated effect of a flue gas contaminant, NO₂, on the deactivation of [P₆₆₆₁₄][Benzim] was investigated and compared to NO. Industrially relevant gas concentrations were used to demonstrate how small amounts of impurities can dramatically change the capability of a sorbent to capture CO₂, and in this particular case a ~60% decrease

in CO₂ capacity was observed. This decrease was corroborated by other experimental techniques and DFT calculations, showing the importance of considering contaminants when designing ionic liquids, or new sorbents in general, for CO₂ capture. Spectroscopic results in combination with DFT calculations showed that NO₂ was predominately strongly physically absorbed on multiple sites, in the form of N₂O₄. This species was then found to undergo heterolytic cleavage resulting in the deactivation of the IL. The ability to investigate the effects of flue gas impurities, individually and competitively, on CO₂ uptake is an important experimental tool in the development of new sorbents and highlights the need for rigorous experimental methods, preferably in tandem with theoretical studies, and the investigation of more complex, realistic multi-component feeds.

Overall, these results show the importance of investigating the effect of flue gas contaminants. Further studies into the feasibility and optimization of ILs in such a process is still required, but a consideration of impurities and sorbent recyclability is an essential factor. Significant improvements in tuning the selectivity and absorption enthalpies of ILs to reversibly capture NO_x or SO₂ at high efficiencies are challenging and alternative methods of removing acidic impurities will still be required (gas scrubbers and traps). Additionally, tuning the basicity of the IL by selecting anions with different pK_a values, presents an interesting opportunity for the pretreatment of waste gas feeds, where contaminants such as NO_x could be reversibly captured.

Acknowledgements

The authors acknowledge funding from the EPSRC under grant no. EP/N009533/1, a multi-disciplinary approach to generating low carbon fuels, carried out in collaboration with the University of Manchester, Queen's University Belfast, Cardiff University and University College London. Open access data can be found via the University of Manchester research

portal. AJG further acknowledges funding from the Department for Employment and Learning. Computing facilities for this work were provided by ARCCA at Cardiff University, HPC Wales, and through membership of the UK's Materials Chemistry Consortium (MCC). Additionally, computing resources were provided by STFC Scientific Computing Department's SCARF cluster. The MCC is funded by the EPSRC (EP/F067496). The UK Catalysis Hub is thanked for resources and support provided via membership of the UK Catalysis Hub Consortium and funded by EPSRC (Grants EP/R026815/1, EP/ K014854/1, and EP/M013219/1).

Supporting Information

The supporting information is available free of charge on the ACS Publications website at: <http://pubs.acs.org>.

Gravimetric results (Figure S1); absorption rig data displayed in Figure 1 (Table S1); NMR data, and $^1\text{H}/^{13}\text{C}$ NMR spectra (Figure S2 and S3, respectively); ATR-IR spectra after the absorption of 1% NO_2 (Figure S4); N 1s XPS spectra (Figure S5); calculated absorption energies (Tables S2 and S3) and grouped Mulliken charges/spin populations for various gases to [P₃₃₃₃][Benzim] (Tables S4 and S5); Potential energy landscape of oxygen transfer from bound NO_2^+ (Figure S6); ATR-IR difference spectra of the absorption of NO_2 and $\text{NO}_2 + \text{CO}_2$ co-feed (Figure S7); ATR-IR spectra showing desorption of the NO_2 , and $\text{NO}_2 + \text{CO}_2$ co-feed (Figure S8); Mechanism depicting the effect of N_2O_4 adsorption on the CO_2 recyclability of [P₆₆₁₄][Benzim] (Figure S9); Potential energy landscape of CO_2/NO absorption (Figure S10); listed Cartesian co-ordinates.

References

1. Khatri, R., Chuang, S., Soong, Y. & Gray, M. Thermal and Chemical Stability of Regenerable Solid Amine Sorbent for CO₂ Capture. *Energy & Fuels* **2006**, *20*, 1514–1520. DOI: 10.1021/ef050402y
2. Ertl, G. & Knoezinger, H. *Handbook of Heterogeneous Catalysis*, vol. 5. (Wiley-VCH, 1997).
3. Gao, J., Wang, S., Zhao, B., Qi, G. & Chen, C. Pilot-scale experimental study on the CO₂ capture process with existing of SO₂: Degradation, reaction rate, and mass transfer. *Energy and Fuels* **2011**, *25*, 5802–5809. DOI: 10.1021/ef2010496
4. Clean Air Technology Centre. *Nitrogen Oxides (NO_x), Why and How They Are Controlled*; EPA 456/F-99-006R; United States Environmental Protection Agency: Research Triangle Park, 1999.
5. European Parliament Directive 2008/50/EC of 21 May 2008 on ambient air quality and cleaner air for Europe [Online]. [Accessed 22 October 2018]. Available at: <https://eur-lex.europa.eu/>.
6. Fostås, B., Gangstad, A., Nenseter, B., Pedersen, S., Sjøvoll, M. & Sørensen, A. L. Effects of NO_x in the flue gas degradation of MEA. *Energy Procedia* **2011**, *4*, 1566–1573. DOI: 10.1016/j.egypro.2011.02.026
7. Supap, T., Shi, H., Idem, R., Gelowitz, D., Campbell, C. & Ball, M. Nitrosamine Formation Mechanism in Amine-Based CO₂ Capture: Experimental Validation. *Energy Procedia* **2017**, *114*, 952–958. DOI: 10.1016/j.egypro.2017.03.1239
8. Magee, P. N. & Barnes, J. M. The production of malignant primary hepatic tumours in the rat by feeding dimethylnitrosamine. *Br. J. Cancer* **1956**, *10*, 114–122. DOI: 10.1038/bjc.1956.15

9. Rogers, R. D. & Seddon, K. R. Ionic Liquids - Solvents of the Future? *Science* **2003**, *302*, 792–793. DOI: 10.1126/science.1090313
10. Greer, A. J., Jacquemin, J. & Hardacre, C. Industrial Applications of Ionic Liquids. *Molecules* **2020**, *25*, 5207. DOI: 10.3390/molecules25215207
11. Blanchard, L. A., Hancu, D., Beckman, E. J. & Brennecke, J. F. Green processing using ionic liquids and CO₂. **1999**, *399*, 28–29. DOI: 10.1038/19887
12. Muldoon, M. J., Aki, S. N. V. K., Anderson, J. L., Dixon, J. K. & Brennecke, J. F. Improving carbon dioxide solubility in ionic liquids. *J. Phys. Chem. B* **2007**, *111*, 9001–9009. DOI: 10.1021/jp071897q
13. Zhang, Y., Zhang, S., Lu, X., Zhou, Q., Fan, W. & Zhang, X. Dual amino-functionalised phosphonium ionic liquids for CO₂ capture. *Chemistry* **2009**, *15*, 3003–3011. DOI: 10.1002/chem.200801184
14. Gurkan, B. E., de la Fuente, J. C., Mindrup, E. M., Ficke, L. E., Goodrich, B. F., Price, E. A., Schneider, W. F. & Brennecke, J. F. Equimolar CO₂ Absorption by Anion-Functionalized Ionic Liquids. *J. Am. Chem. Soc.* **2010**, *132*, 2116–2117. DOI: 10.1021/ja909305t
15. Wang, C., Luo, X., Luo, H., Jiang, D. E., Li, H. & Dai, S. Tuning the basicity of ionic liquids for equimolar CO₂ capture. *Angew. Chemie - Int. Ed.* **2011**, *50*, 4918–4922. DOI: 10.1002/anie.201008151
16. Seo, S., Quiroz-Guzman, M., DeSilva, M. A., Lee, T. B., Huang, Y., Goodrich, B. F., Schneider, W. F. & Brennecke, J. F. Chemically Tunable Ionic Liquids with Aprotic Heterocyclic Anion (AHA) for CO₂ Capture. *J. Phys. Chem. B* **2014**, *118*, 5740–5751. DOI: 10.1021/jp502279w

17. Gohndrone, T. R., Bum Lee, T., DeSilva, M. A., Quiroz-Guzman, M., Schneider, W. F. & Brennecke, J. F. Competing Reactions of CO₂ with Cations and Anions in Azolide Ionic Liquids. *ChemSusChem* **2014**, *7*, 1970–1975. DOI: 10.1002/cssc.201400009
18. Taylor, R., McCrellis, C., McStay, C., Jacquemin, J., Hardacre, C., Mercy, M., Bell, R. G. & de Leeuw, N. H. CO₂ Capture in Wet and Dry Superbase Ionic Liquids. *J. Solution Chem.* **2015**, *44*, 511–527. DOI: 10.1007/s10953-015-0319-z
19. Wang, C., Cui, G., Luo, X., Xu, Y., Li, H. & Dai, S. Highly efficient and reversible SO₂ capture by tunable azole-based ionic liquids through multiple-site chemical absorption. *J. Am. Chem. Soc.* **2011**, *133*, 11916–11919. DOI: 10.1021/ja204808h
20. Cui, G., Zheng, J., Luo, X., Lin, W., Ding, F., Li, H. & Wang, C. Tuning anion-functionalized ionic liquids for improved SO₂ capture. *Angew. Chemie - Int. Ed.* **2013**, *52*, 10620–10624. DOI: 10.1002/anie.201305234
21. Chen, K., Lin, W., Yu, X., Luo, X., Ding, F., He, X., Li, H. & Wang, C. Designing of anion-functionalized ionic liquids for efficient capture of SO₂ from flue gas. *AIChE J.* **2015**, *61*, 2028–2034. DOI: 10.1002/aic.14793
22. Chen, K., Shi, G., Zhou, X., Li, H. & Wang, C. Highly Efficient Nitric Oxide Capture by Azole-Based Ionic Liquids through Multiple-Site Absorption. *Angew. Chemie Int. Ed.* **2016**, *55*, 14364–14368. DOI: 10.1002/anie.201607528
23. Cao, N., Gan, L., Xiao, Q., Lv, X., Lin, W., Li, H. & Wang, C. Highly Efficient and Reversible Nitric Oxide Capture by Functionalized Ionic Liquids through Multiple-Site Absorption. *ACS Sustain. Chem. Eng.* **2020**, *8*, 2990-2995. DOI: 10.1021/acssuschemeng.9b07657
24. Sun, Y., Ren, S., Hou, Y., Zhang, K., Zhang, Q. & Wu, W. Highly Reversible and

- Efficient Absorption of Low-Concentration NO by Amino-Acid-Based Ionic Liquids. *ACS Sustain. Chem. Eng.* **2020**, *8*, 3283-3290. DOI: 10.1021/acssuschemeng.9b06923
25. Zhai, R., He, X., Mei, K., Chen, K., Cao, N., Lin, W., Li, H. & Wang, C. Ultrahigh Nitric Oxide Capture by Tetrakis(azolyl)borate Ionic Liquid through Multiple-Sites Uniform Interaction. *ACS Sustain. Chem. Eng.* **2021**, *9*, 3357-3362. DOI: 10.1021/acssuschemeng.1c00024
26. Taylor, S. F. R., McClung, M., McReynolds, C., Daly, H., Greer, A. J., Jacquemin, J. & Hardacre, C. Understanding the Competitive Gas Absorption of CO₂ and SO₂ in Superbase Ionic Liquids. *Ind. Eng. Chem. Res.* **2018**, *57*, 17033–17042. DOI: 10.1021/acs.iecr.8b03623
27. Greer, A. J., Taylor, S. F. R., Daly, H., Quesne, M., Catlow, C. R. A., Jacquemin, J. & Hardacre, C. Investigating the Effect of NO on the Capture of CO₂ Using Superbase Ionic Liquids for Flue Gas Applications. *ACS Sustain. Chem. Eng.* **2019**, *7*, 3567–3574. DOI: 10.1021/acssuschemeng.8b05870
28. Duan, E., Guo, B., Zhang, D., Shi, L., Sun, H. & Wang, Y. Absorption of NO and NO₂ in Caprolactam Tetrabutyl Ammonium Halide Ionic Liquids. *J. Air Waste Manage. Assoc.* **2011**, *61*, 1393–1397. DOI: 10.1080/10473289.2011.623635
29. Li, X., Zhang, L., Li, L., Hu, Y., Liu, J., Xu, Y., Luo, C. & Zheng, C. NO Removal from Flue Gas Using Conventional Imidazolium-Based Ionic Liquids at High Pressures. *Energy & Fuels* **2018**, *32*, 6039–6048. DOI: 10.1021/acs.energyfuels.8b00154
30. Kunov-Kruse, A. J., Thomassen, P. L., Riisager, A., Mossin, S. & Fehrmann, R. Absorption and Oxidation of Nitrogen Oxide in Ionic Liquids. *Chem. - A Eur. J.* **2016**, *22*, 11745–11755. DOI: 10.1002/chem.201601166

31. Oster, K., Goodrich, P., Jacquemin, J., Hardacre, C., Ribeiro, A. P. C. & Elsinawi, A. A new insight into pure and water-saturated quaternary phosphonium-based carboxylate ionic liquids: Density, heat capacity, ionic conductivity, thermogravimetric analysis, thermal conductivity and viscosity. *J. Chem. Thermodyn.* **2018**, *121*, 97–111. DOI: 10.1016/j.jct.2018.02.013
32. Frisch, M. J., Trucks, G. W., Schlegel, H. B., Scuseria, G. E., Robb, M. A., Cheeseman, J. R., G. Scalmani, V. B., Mennucci, B., Petersson, G. A., Nakatsuji, H., Caricato, M., Li, X., Hratchian, H. P., Izmaylov, A. F., Bloino, J., Zheng, G., Sonnenberg, J. L., Hada, M., Ehara, M., Toyota, K., Fukuda, R., Hasegawa, J., Ishida, M., Nakajima, T., Honda, Y., Kitao, O., Nakai, H., Vreven, T., Montgomery, J. A., Peralta, J. E., Ogliaro, F., Bearpark, M., Heyd, J. J., Brothers, E., Kudin, K. N., Staroverov, V. N., Kobayashi, R., Normand, J., Raghavachari, K., Rendell, A., Burant, J. C., Iyengar, S. S., Tomasi, J., Cossi, M., Rega, N., Millam, J. M., Klene, M., Knox, J. E., Cross, J. B., Bakken, V., Adamo, C., Jaramillo, J., Gomperts, R., Stratmann, R. E., Yazyev, O., Austin, A. J., Cammi, R., Pomelli, C., Ochterski, J. W., Martin, R. L., Morokuma, K., Zakrzewski, V. G., Voth, G. A., Salvador, P., Dannenberg, J. J., Dapprich, S., Daniels, A. D., Farkas, Foresman, J. B., Ortiz, J. V, Cioslowski, J. & Fox, D. J. Gaussian 09, Revis. A.02, Gaussian, Inc., Wallingford CT, 200.
33. Sahu, S., Quesne, M. G., Davies, C. G., Dürr, M., Ivanović-Burmazović, I., Siegler, M. A., Jameson, G. N. L., De Visser, S. P. & Goldberg, D. P. Direct observation of a nonheme iron(IV)-oxo complex that mediates aromatic C-F hydroxylation. *J. Am. Chem. Soc.* **2014**, *136*, 13542–13545. DOI: 10.1021/ja507346t
34. Neu, H. M., Yang, T., Baglia, R. A., Yosca, T. H., Green, M. T., Quesne, M. G., de Visser, S. P. & Goldberg, D. P. Oxygen-Atom Transfer Reactivity of Axially Ligated

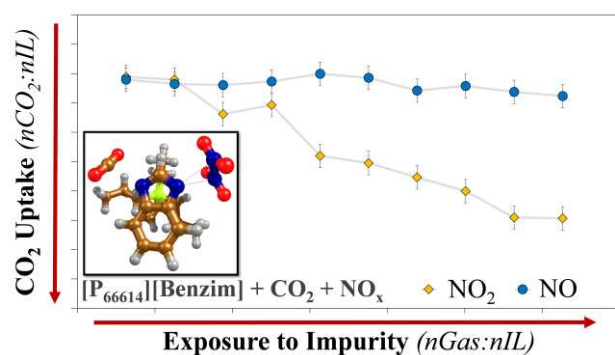
- Mn(V)–Oxo Complexes: Evidence for Enhanced Electrophilic and Nucleophilic Pathways. *J. Am. Chem. Soc.* **2014**, *136*, 13845–13852. DOI: 10.1021/ja507177h
35. Timmins, A., Quesne, M. G., Borowski, T. & de Visser, S. P. Group Transfer to an Aliphatic Bond: A Biomimetic Study Inspired by Nonheme Iron Halogenases. *ACS Catal.* **2018**, *8*, 8685–8698. DOI: 10.1021/acscatal.8b01673
36. Mercy, M., Rebecca Taylor, S. F., Jacquemin, J., Hardacre, C., Bell, R. G. & De Leeuw, N. H. The addition of CO₂ to four superbase ionic liquids: a DFT study. *Phys. Chem. Chem. Phys.* **2015**, *17*, 28674–28682. DOI: 10.1039/c5cp05153c
37. Zhurko, G. & Zhurko, D. Chemcraft Program. Academic version 1.5. **2004**.
38. Grimme, S., Antony, J., Ehrlich, S. & Krieg, H. A consistent and accurate ab initio parametrization of density functional dispersion correction (DFT-D) for the 94 elements H–Pu. *J. Chem. Phys.* **2010**, *132*, 1541040. DOI: 10.1063/1.3382344
39. Polzonetti, G., Alnot, P. & Brundle, C. R. The adsorption and reactions of NO₂ on the Ag(111) surface. I. XPS/UPS and annealing studies between 90 and 300 K. *Surf. Sci.* **1990**, *238*, 226–236. DOI: 10.1016/0039-6028(90)90080-r
40. Sysoev, V. I., Okotrub, A. V., Gusel'nikov, A. V., Smirnov, D. A. & Bulusheva, L. G. In situ XPS Observation of Selective NO_x Adsorption on the Oxygenated Graphene Films. *Phys. status solidi* **2018**, *255*, 17002671–17002675. DOI: 10.1002/pssb.201700267
41. Ruiz-Soria, G., Pérez Paz, A., Sauer, M., Mowbray, D. J., Lacovig, P., Dalmiglio, M., Lizzit, S., Yanagi, K., Rubio, A., Goldoni, A., Ayala, P. & Pichler, T. Revealing the Adsorption Mechanisms of Nitroxides on Ultrapure, Metallicity-Sorted Carbon Nanotubes. *ACS Nano* **2014**, *8*, 1375–1383. DOI: 10.1021/nn405114z

42. Koch, T. G., Horn, A. B., Chesters, M. A., McCoustra, M. R. S. & Sodeau, J. R. A low-temperature reflection-absorption infrared spectroscopic study of ultrathin films of dinitrogen tetroxide and dinitrogen pentoxide on gold foil. *J. Phys. Chem.* **1995**, *99*, 8362–8367. DOI: 10.1021/j100020a072
43. Wang, J. & Koel, B. E. IRAS Studies of NO₂, N₂O₃, and N₂O₄ Adsorbed on Au(111) Surfaces and Reactions with Coadsorbed H₂O. *J. Phys. Chem. A* **1998**, *102*, 8573–8579. DOI: 10.1021/jp982061d
44. Cataldo, F., Compagnini, G., D’Urso, L., Mita, V., Strazzulla, G., Ursini, O. & Angelini, G. Adsorption of dinitrogen tetroxide (N₂O₄) on multi-walled carbon nanotubes (MWCNTs). *Fullerenes Nanotub. Carbon Nanostructures* **2008**, *16*, 154–164. DOI: 10.1080/15363830801888123
45. Pidko, E. A., Mignon, P., Geerlings, P., Schoonheydt, R. A. & Van Santen, R. A. A periodic DFT study of N₂O₄ disproportionation on alkali-exchanged zeolites X. *J. Phys. Chem. C* **2008**, *112*, 5510–5519. DOI: 10.1021/jp077063p
46. Lignell, H., Varner, M. E., Finlayson-Pitts, B. J. & Benny Gerber, R. Isomerization and ionization of N₂O₄ on model ice and silica surfaces. *Chem. Phys.* **2012**, *405*, 52–59. DOI: 10.1016/j.chemphys.2012.06.006
47. Yeadon, D. J., Jacquemin, J., Plechkova, N. V., Maréchal, M. & Seddon, K. R. Induced Protic Behaviour in Aprotic Ionic Liquids by Anion Basicity for Efficient Carbon Dioxide Capture. *ChemPhysChem* **2020**, *21*, 1369–1374. DOI: 10.1002/cphc.202000320
48. Busca, G. & Lorenzelli, V. Infrared study of the adsorption of nitrogen dioxide, nitric oxide and nitrous oxide on hematite. *J. Catal.* **1981**, *72*, 303–313. DOI: 10.1016/0021-

9517(81)90013-0

49. Weston, R. E. & Brodasky, T. F. Infrared Spectrum and Force Constants of the Nitrite Ion. *J. Chem. Phys.* **1957**, 27, 683–689. DOI: 10.1063/1.1743814
50. Gatehouse, B. M. A survey of the infrared spectra of NO₂ in metal complexes. *J. Inorg. Nucl. Chem.* **1958**, 8, 79–86. DOI: 10.1016/0022-1902(58)80167-0

TOC



Synopsis

The mechanism of NO₂ absorption by a superbase ionic liquid is investigated to understand the recyclability of CO₂ capture systems.